ESTIMATED REFRACTIVE INDICES OF CALCITE, DOLOMITE, AND MAGNESITE: ~0.3-500 μm.

T.L. Roush, NASA Ames Research Center, Moffett Field, CA 94035, Ted.L.Roush@nasa.gov

Introduction: Carbonate minerals are germane to questions involving volatile and climate history on Mars [e.g., 1-2]. In particular, the abundance of carbonate-bearing minerals can provide broad useful bounds on the amount of CO_2 out-gassed into the atmosphere over its history and their spatial distribution and mineralogy can yield constraints on the environments in which they were produced. Earth-based, orbital, and landed spectral observations provide evidence for the presence of carbonates in the Martian environment [3-6]. Infrared observations made from spacecraft near Mars were interpreted to indicate the presence of carbonates. [6] associated the carbonates with the surface dust and interpreted the mineralogy as being consistent with magnesite ($MgCO_3$). Near-infrared observations from Mars orbit have been interpreted to suggest magnesite outcrops in restricted locations [7-9].

Quantitative estimates of the abundance of carbonates on Mars range from 0-3% [3], 2-5% [6], less than a few percent [10], and <10% [8]. With the growing evidence for magnesite on Mars additional quantitative estimates can be provided via theoretical modeling of the reflectance from the Martian surface.

Calcite ($CaCO_3$) and dolomite ($(Ca,Mg)CO_3$) are identified in Asian dust [2-17%], [10] and calcite in Saharan dust [~8-10% [12-15]. The importance of optical constants at visible and near-infrared wavelengths as proxies for estimating the effects at infrared wavelengths, has been investigated [15].

The growing evidence for Mg-carbonates on Mars, the presence of calcite and dolomite in terrestrial aerosols, and general lack of optical constants for these materials in the visible- to mid-infrared (VMIR, ~0.3-6 μm) has motivated the current effort to estimate the optical constants of calcite, dolomite, and magnesite in the VMIR.

Methodology: Using reflectance measurements of calcite, dolomite, and magnesite from a variety of online spectral libraries [16-18]. For each of the carbonates all the libraries were searched and available data cataloged. The bulk of these samples were eliminated due to the availability of only a single grain size, the presence of spectral features associated with other materials, the presence of odd spectral behavior, and/or lack of data at wavelengths long enough to overlap with the infrared data. For magnesite, nine possible samples were identified, and only a single sample, having two grain sizes was used. Additionally, a continuum as used to eliminate spectral features due to Fe^{2+} prior to determination of the refractive indices. For dolomite, nine possible samples were identified, and only a single sample, having three grain sizes was used. For calcite, fifty six possible samples were identified, and two samples, having five grain sizes were used.

A radiative transfer model for the visible and mid-infrared wavelengths (~0.3-6 μm) was used to provide an estimate of the imaginary index of refraction, k. Input parameters include: 1) reflectance spectrum, lab viewing geometry, sample particle size (from lab documentation), sample solid density (from literature), real index of refraction (n, initially a constant value calculated as an average from several literature values of the ordinary and extraordinary axes), and a convergence criterion (10^{-6} was used). The general process is illustrated in Fig. 1.

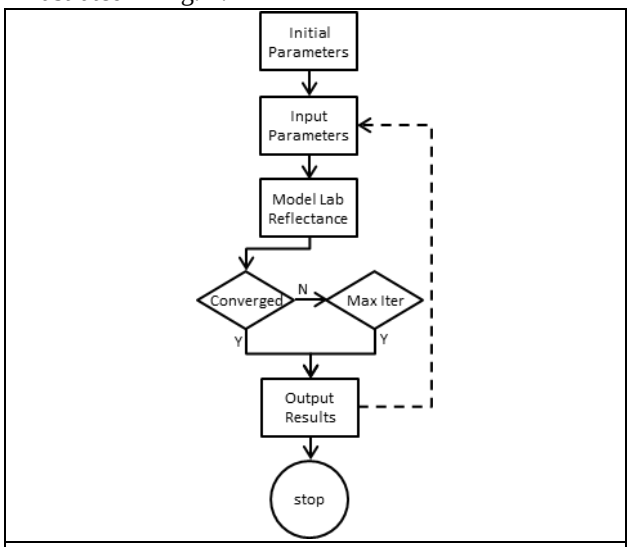

Figure 1. Schematic diagram of the process used to estimate k.

The resulting k values are combined with literature values at longer wavelengths [19] by fitting a quadratic to join the shorter and longer wavelength k-values in the 5.5-6 μm region. The combined data are used in a subtractive Kramers-Kronig analysis to estimate n, as described in [20]. This iterative process is captured in Fig. 2.

Results: The iterative approach illustrated in Fig. 2 was repeated until the real and imaginary indices did not change significantly between successive iterations.

This nominally required three iterations between the Hapke and SKK applications.

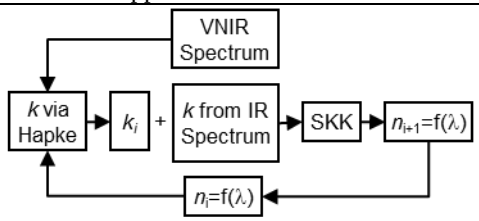

Figure 2. Schematic diagram of iterative use of Hapke calculations and subtractive Kramers-Kronig analysis (SKK) to determine the wavelength dependence of n.

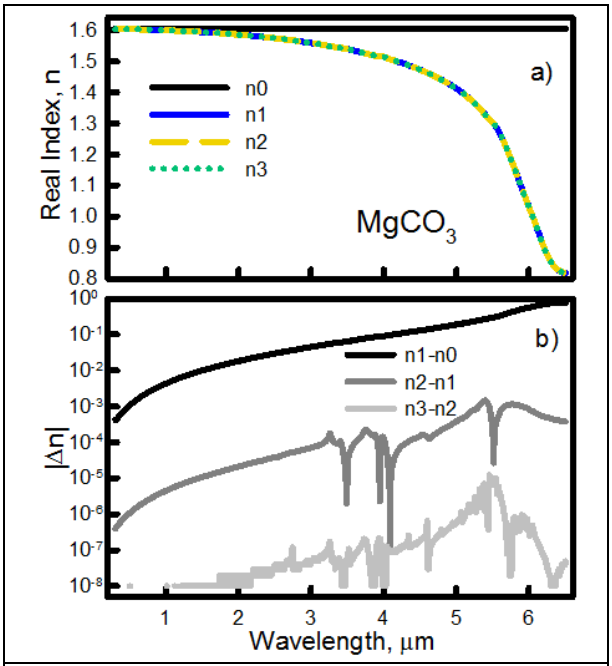

Figure 3. Magnesite refractive index as a function of iteration. (a) real index, n, black line is the initial estimate where n=constant and other colors represent subsequent values for n=f(λ). (b) Difference |Δn| between successive iterations for n. By the third iteration (light gray line) the differences are < ~10^{-6}. Values of |Δn| = 0 are not shown on the logarithmic scale and result in a gap in the curves.

As shown in Fig. 3, differences are typically <10^{-5} for n between iteration 3 and 2. The greatest differences in the n was the transition from the initial assumption of a n = constant to the results of the first SKK analyses where n = *f(λ)*. Fig. 4 shows that differences are typically <10^{-6} for k between iterations 3 and 2. The greatest differences observed for k were in the region where imaginary indices were combined with the longer wavelength data. Similar results are seen for n and k of calcite and dolomite.

Conclusions: Final results for all three carbonates will be submitted publication and to the PDS.

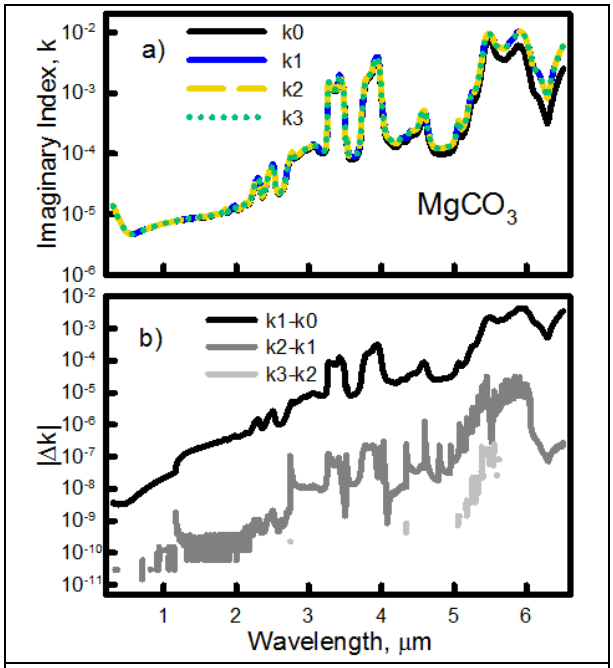

Figure 4. Magnesite refractive index as a function of iteration. (a) imaginary index, k, black line is the initial estimate with n=constant and other colors represent subsequent values for k with n=f(λ). (b) Difference |Δk| between successive iterations for k. In the third iteration (light gray line) differences are < ~10^{-7}. Values of |Δk| = 0 are not shown on the logarithmic scale and result in gaps in the curves.

Acknowledgements: This research has been enabled via support from NASA's PDART program.

References: [1] Pollack, et al., *Icarus 71*, 1987 [2] Fanale et al., Mars, U. Az. 1992 [3] Pollack et al. *JGR 95* 1990 [4] Lellouch et al. *PSS 48*, 1992 [5] Calvin et al. *JGR 99*, 1994 [6] Bandfield et al. *Science 301*, 2003 [7] Ehlman et al. *Science 322*, 2008 [8] Palomba et al. *Icarus 203*, 2009 [9] Michaelski and Niles *Nat. Geosci., 3*, 2010 [10] Bibring et al. *Science 307*, 2005 [11] Jeong, *JGR 113*, 2008 [12] Glaccum and Prospero *Mar. Geol. 37*, 1980 [13] Avila et al. *JGR 102*,1997 [14] Reid et al. *JGR 108*, 2003 [15] Hansell et al. *Atmos. Chem. Phys., 11*, 2011 [16] Baldridge et al. *Rem. Sens. Environ., 113*, 2009 [17] NASA RELAB facility, Brown University, RELAB [18] Planetary Spectrophotometer Facility, PSF [19] Hellewege et al. *Zeit. Physik 232*, 1971 [20] Roush et al. *JGR 112*, 2007.